Measurement of Ferret Brain Tissue Stiffness *in vivo* Using MR Elastography

Y. V. Chang[1], Y. A. Feng[1], E. H. Clayton[1], and P. V. Bayly[1]
[1]Mechanical Engineering, Washington University, St. Louis, MO, United States

Introduction Characterizing the mechanical properties of brain tissue is critical in understanding traumatic brain injury (1) and the mechanisms of cortical folding (2,3). Ferret brains provide an ideal animal model for this purpose because of the postnatal development of surface folds (4-6). MR elastography (MRE) has been used as a powerful tool to non-invasively measure the mechanical properties of biological tissues (7,8). In this work we present our initial experience of characterizing the ferret brain tissue stiffness using MRE at several different frequencies. Since ferret brains contain significant whiter matter compared to rodents (9,10), MRE of the ferret brain can potentially be applied to study the mechanical changes of the brain associated with white matter diseases (e.g., multiple sclerosis) or axonal damage (11).

Methods Experiments were performed on a 4.7 T superconducting magnet (Oxford) controlled by the Varian INOVA-UNITY console. Two female adult ferrets (Marshall Bioresources) were anesthetized with 1.5% isofluorane during experiments with the pulse rate and oxygen saturation level monitored by a pulse oximeter (Kent Scientific). All the experimental protocols were approved by our institutional review board. Harmonic motion was generated by a TTL-equipped function generator and a voltage amplifier, which drives a piezo-ceramic actuator (APA150M-NM, Cedrat Technologies) connected to a Delrin bite bar (Fig.1). During experiments the ferret head was secured on the bite bar using the nose cone to ensure proper transmission of the shear wave to the brain. A custom-built, low-pass birdcage quadrature coil of 8 rungs (length: 6.5 cm, diameter: 7.6 cm) was used for both RF transmitting and receiving. Data were collected using a custom gradient-echo sequence with harmonic motion-encoding gradient waves added. Measurements were made at 400, 800 and 1200 Hz. At each frequency images were collected with both polarities of the motion-encoding gradients. For each gradient polarity the acquisitions were synchronized to the actuator vibration to ensure consistent phase encoding of tissue displacement. Images were acquired at 4 different phase shifts ($\phi = 0, \pi/2, \pi, 3\pi/2$). 4, 16, and 24 motion encoding cycles with peak gradient amplitude of 15 G/cm were used at 400, 800, and 1200 Hz, respectively. The imaging parameters include: TR/TE = 200/13.75 ms at 400 Hz and TR/TE = 300/23 ms at 800 and 1200 Hz; 11 contiguous slices; 0.5 mm isotropic voxels; 50 kHz bandwidth. Measurements were performed in all three directions. Data analysis was described in detail in previous work (10). In brief, the displacement fields $\boldsymbol{u}(x, y, t)$ were first obtained by converting the unwrapped (Phase Vision) phase maps from the division of the positive- and negative-polarity images; the fundamental harmonics (Fig. 3(a)) at each pixel $\boldsymbol{U}(x, y, \omega)$ was calculated by Fourier transform in the time domain, followed by spatial smoothing using a Butterworth bandpass filter (in: 0.08 mm^{-1}, out: 0.33 mm^{-1}) (Fig. 3(b)). The finite difference scheme was used to approximate the Laplacian field $\nabla^2\boldsymbol{U}(x, y, \omega)$. The storage modulus G' and the loss modulus G'' were calculated by inverting the linear isotropic homogenous material equation of motion, $(G' + iG'')\nabla^2\boldsymbol{U}(x, y, \omega) = -\rho\omega^2\boldsymbol{U}(x, y, \omega)$, where ρ is tissue density. Voxels with normalized residual errors (NRE) higher than 0.8 or negative values of G' are discarded.

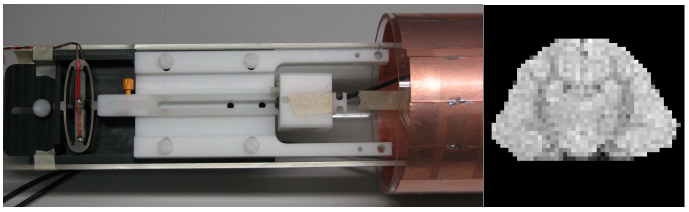

Figure 1 The ferret MRE setup, including the actuator, the nose cone, the bite bar, and the RF coil. On the right is a T_2-weighted anatomical image of the ferret brain.

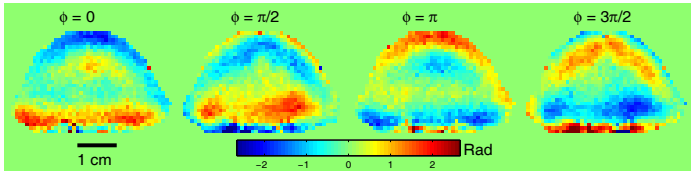

Figure 2 A representative set of unwrapped phase images acquired at different phase shifts at 400 Hz.

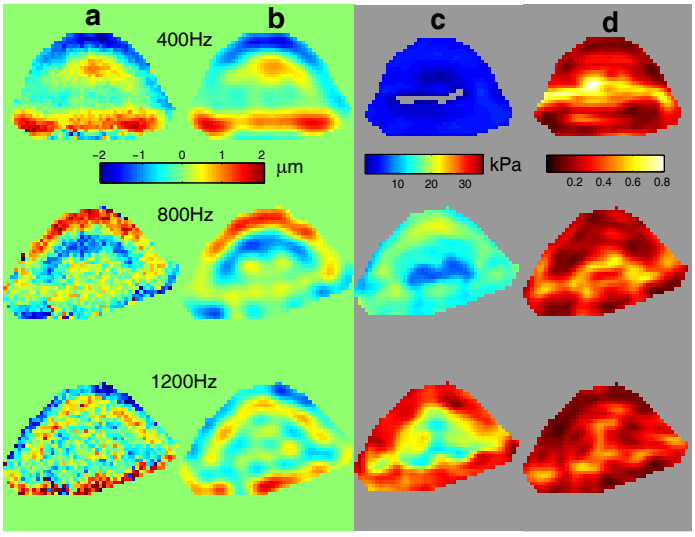

Figure 3 The real part of the raw (a) and filtered (b) displacement fields, the maps of the storage modulus (c) and normalized residual error (d) at 400 (top), 800 (middle), and 1200 (bottom) Hz.

Results A T_2-weighted anatomical image of the ferret brain is shown on the right of Fig. 1. A representative set of unwrapped phase images at different phase shifts at 400 Hz is shown in Fig. 2. The real components of the displacement fields, obtained by Fourier transform of the phase images represented in Fig. 2, before and after spatial filtering, are shown in Fig. 3(a) and (b), respectively, at 400, 800 and 1200 Hz. Maps of storage modulus and NRE at all frequencies are shown in Fig. 3(c) and (d). The average storage modulus at 400, 800 and 1200 Hz are 3.6 ± 1.3, 11 ± 3, and 21 ± 6 kPa, respectively.

Discussion The ferret brain (like mouse and human) appears viscoelastic, and exhibits significant increase in stiffness with frequency. Our measurements suggest that the ferret brain may be slightly stiffer than the mouse brain (10) but softer than the human brain, both measured at similar frequencies (12). From this observation, we speculate that the brain tissue stiffness may be weakly correlated with brain size. This would need to be carefully confirmed, but we speculate further that a larger brain with less support from the skull would need higher stiffness to hold its shape. Our results also show that spatial variations in stiffness are difficult to detect in ferrets, particularly at frequencies below 1000 Hz and the corresponding longer wavelengths. If contrast-noise ratio can be maintained, MRE at higher frequencies may be able to detect stiffness variations between white and gray matter.

Conclusion We have demonstrated the feasibility of *in vivo* MRE measurement of ferret brain tissue stiffness. At 400 Hz, the ferret brain appears slightly stiffer than the mouse brain and softer than the human brain measured at similar frequencies.

Acknowledgments Work supported by NIH grant R21EB005834.

References (1) Bayly PV et al. J Biomech 2006;39:1086 (2) Van Essen DC et al. Nature 1997;385:313 (3) Xu G et al. J Biomech Eng 2010;132:071013 (4) Barnette AR et al. Pediatric Research 2009;66:80 (5) Kroenke CD et al. Cerebral Cortex 2009;19:2916 (6) Knutsen AK et al. J Biomech Eng 2010;132:101004 (7) Muthupillai R et al. Science 1995;269:1854 (8) Atay SM et al. J Biomech Eng 2008;130:021013 (9) Diguet E et al. ISMRM 2009;715 (10) Clayton EH et al. ISMRM 2010;633 (11) Mac Donald CL et al. J Neurosci 2007;27:11869 (12) McCracken PJ et al. MRM 2006;53:628